DISRUPTION STUDIES ON ASDEX UPGRADE

G. Pautasso, S. Egorov [1], K.H. Finken [2], O. Gruber, A. Herrmann, C.J. Fuchs, M. Maraschek, G. Neu, Y. Nakamura [3], V. Rohde, A. Savtchkov [2], S. Schweizer, U. Seidel, B. Streibl, Ch. Tichmann and the ASDEX Upgrade Team.

Max-Planck-Institut für Plasmaphysik, EURATOM Association, 85748 Garching, Germany

[1] Technical University, St. Petersburg, Russia.

[2] Institut für Plasmaphysik, Forschungszentrum Jülich, Association KFA-EURATOM, Member of the Trilateral euregio Cluster (TEC), 52425 Jülich, Germany.

[3] Japan Atomic Energy Research Institute, Naka-machi, Naka-gun, Ibaraki 311-0193, Japan.

1. Introduction.

Disruptions generate large thermal and mechanical stresses on the tokamak components and are occasionally responsible for damages to the machine. For a future reactor disruptions have a significant impact on the design since all loading conditions must be analyzed in accordance with stricter design criteria (due to safety or difficult maintenance). Therefore the uncertainties affecting the predicted stresses must be reduced as much as possible with a more comprehensive set of measurements and analyses in this generation of experimental machines, and avoidance/predictive methods must be developed further.

Disruption studies on ASDEX Upgrade are focused on these subjects, namely on:

(1) understanding the physical mechanisms leading to this phenomenon in order to learn to avoid it or to predict its occurrence and to mitigate its effects;

(2) analyzing the effects of disruptions on the machine to determine the functional dependence of the thermal and mechanical loads upon the discharge parameters. This allows, firstly, to dimension or reinforce the machine components to withstand these loads and, secondly, to extrapolate them to tokamaks still in the design phase;

(3) learning to mitigate the consequence of disruptions, i.e. thermal loads, mechanical forces and runaways with injection of impurity pellets or gas.

This paper is focused on most recent results concerning points (2) and (3), i.e. on the analysis of the degree of asymmetry of the forces and on the use of impurity puff for mitigation. For recent developments on point (1) see Ref. [1]; for recent experiments on the *neutral point* see Ref. [2].

2. Asymmetric halo currents.

The halo currents, which are the major causes of mechanical stresses on the machine during disruptions, are known to be toroidally asymmetric. This fact was first reported by JET and then confirmed by the other major tokamaks. This asymmetry manifests itself often as a combination of n=0 and n=1 components; in other cases it has a less definable structure.

In Asdex Upgrade plasmas the n=1 perturbation of the halo current [3] is always clearly seen in density limit disruptions at $|q_{95}| \simeq 5 - 6$ and in disruptions following a VDE (with $|q_{95}| \simeq 2$ at the disruption time). The n=1 structure is always clearly correlated with a reconnection phenomenon seen by several diagnostics and appears when $|q_{cyl}|$ approaches or becomes smaller than 2 ($|q_{cyl}|$ is an approximate estimation of q_{95} after disruption, when the equilibrium reconstruction program fails to deliver reliable values of q_{95}). The SXR emission drops abruptly after a strong kink-like movement of the plasma center, the H_α signal and the heat load measured by

the thermography show a large flux of particles and heat to the structures; the Mirnov coils see the n=1 structure of a mode. The Mirnov coils in the lower part of the vessel are saturated but the poloidal arrays of halo current measurements show a poloidal structure consistent with a m=1 poloidal mode number of the n=1 structure. The n=1 structure does not necessarily rotate.

The role of q_{cyl} in the appearance of the n=1 structure (Fig. 1 (b)) is clearly seen in Fig. 1 (a) and confirmed by the scatter plot in Fig. 2 showing the local toroidal peaking factor *tpf* (ratio of maximum to toroidally averaged halo current measured at the DUMa tiles, shown in Fig. 1 (c)), as function of q_{cyl} at the time of the max halo current. The *tpf* reaches its maximum for $q_{cyl} \sim 2$. The *tpf* also has a maximum for $4 < |q_{95}| < 5.5$; for shots which disrupt with a small $|q_{95}| \simeq 2 - 3$ in the midplane the current quench is rather fast and turbulent; the n=1 mode is not seen and the *tpf* at the time of max halo current remains relatively small.

The n=1 halo structure is also suppressed or its amplitude reduced with the injection of killer pellets. In disruption-softening experiments carried out with impurity puffing, instead, the n=1 is still clearly observed (in spite of the significant reduction of the average toroidal halo current). This suggests that a reduction of the plasma current peaking at the center (which can be assumed after pellet injection) reduces the *tpf*.

The several observations reported above are consistent with the following picture. The m=1, n=1 structure of the halo current has to grow on the q=1 surface; at the time of the asymmetry growth the q_{cyl} is ~ 2. It is not clear which role the q=2 surface plays in triggering the [1,1] mode. The significant role of the q=1 surface is consistent with parametric studies of the current profiles and with the following facts: when the toroidal plasma current profile is flat then the q=1 surface is small or absent and therefore (1) after killer-pellet, (2) in turbulent post-disruption phases and (3) in plasmas with a fast current quench (no reheating, no repeaking of the flat post-thermal-quench current profile, absence of SXR emission) the [1,1] structure is not seen.

3. On the toroidal asymmetry of the forces on the vessel.

Large radial vessel displacements up to 6 mm are observed, at least up to now, only on JET [4]. The toroidally asymmetric vessel movement is accompanied by a n=1 tilt of the whole plasma seen in the magnetic reconstruction of the plasma position. This peculiarity and its relevance in the design of the ITER vessel has motivated a careful analysis of the mechanical forces on ASDEX Upgrade.

3.1 Diagnostics for the measurements of forces.

The tokamak Asdex Upgrade is equipped with several diagnostics, which indirectly measure the mechanical forces on different components.

The vacuum vessel is suspended through eight rods at an external supporting structure. The rods are $\pi/4$ radiants apart (in sector 1, 3, 5 etc.) and each of the rod is equipped with a strain gauge. The sampling rate of this diagnostic is rather high (2 or 5 kHz) compared with the main oscillation frequency of the vessel in the vertical direction (of the order of 16 Hz) and allows a clear time resolution of the vessel dynamics. The vessel is also equipped with displacement gauges, which measure its radial and vertical movement at the equatorial plane at four toroidal positions, 90° apart (in sector 1, 5, 9 and 13). These measurements have a sampling rate of 200 Hz. The following analysis has required a thorough calibration of the described gauges.

3.2 Vertical forces measured at the vessel suspension rods.

The analysis was done over the shot range 15200-16000 for plasma currents up to 1 MA (one disruption at 1.2 MA) and toroidal magnetic field in the range 1.2-2.9 Tesla. The database contains one hundred disruptions in flat-top followed by vertical displacement, shortly VD.

With VDE we indicate instead the vertical displacement event ending with a disruption.

The time history of the eight strain gauges at the vessel suspension rods are show in Fig. 3 for a downwards VDE. We use the following notation: $F_z = \sum_n F_{z(n)}$ is the total vertical force acting on the vessel; $F_{z(n)}$ with n= 1,2...8 is the force measured by the strain gauge mounted at the n-th rod and located in sector 2n;

The amplitude of the forces measured at the rods can reach values above 300 kN at plasma currents of 0.8-1 MA; in slow VDEs downwards, with growth rates of the order of 100 ms, the negative force reached the 500 kN. The max and min forces do not simply scale with I_p^2 or $I_p * B_t$; as a *rule of thumb,* we derive that $|F_z| =< 250$ kN/(MA Tesla). The toroidal asymmetries of the vertical forces, as measured at the rods, are typically less than 20 % and in average about 10 %.

3.3 Vertical and radial displacement at the vessel midplane.

The vertical displacement of the vessel (d_z), measured at the vessel midplane has a time behavior similar to that measured by the strain gauges at the suspension rods. The maximum vertical displacement is about 0.7 mm, in both positive and negative vertical direction (Fig. 4).

An example of the time history of the vessel radial displacements is shown in Fig. 4. The largest net radial displacements observed in the shot period analized are of the order of 0.2 mm and therefore significantly small. The net radial displacement of the vessel is calculated as

$$d_R = \sqrt{d_{9 \to 1}^2 + d_{13 \to 5}^2}$$

$d_{9 \to 1} = (d_{R(1)} - d_{R(9)})/2$ for the displacement in the direction from sector 9 to sector 1,

$d_{13 \to 5} = (d_{R(5)} - d_{R(13)})/2$ for the displacement in the direction from sector 13 to sector 5.

The vessel was intentionally laterally displaced by applying a known force to establish the correspondence between applied force and radial displacement; this was found to be approximately linear and amount to 0.014 mm/kN for a statically applied force. The largest radial displacement observed during disruptions is of 0.24 mm and corresponds to a statically applied radial force of 17 kN; but since the forces during disruptions act for a fraction of the oscillation period of the vessel, the shortly applied force could be up to one order of magnitude larger. It is interesting to point out that the discharges with the largest radial displacement are disruptions following VDE as in JET.

The relation between asymmetries of halo currents and vessel displacements has not been clarified yet.

4. Mitigation of disruptions with impurity puff.

A fast valve system, developed by the authors of the Forschungszentrum in Jülich [5], has been used on ASDEX Upgrade for a series of experiments. The fast valve can inject up to a few hundreds mbarl of impurity gas within 1 ms. Experiments were carried out with up to 180 mbarl (3 bar * 60 cm^3 = 4.5 10^{21} particles, of which 2/3 were actually injected) of Helium (He), Neon (Ne) and Argon (Ar) in limiter and divertor plasmas. The purpose of the present experiment was to look for an impurity gas puff regime which can routinely be used on ASDEX Upgrade for disruptions mitigation (in conjunction with a disruption prediction system). We compared the performance of He, Ne and Ar in reducing the mechanical forces and thermal loads on the machine after disruptions and choose optimal gas quantity and pressure taking into account that: 1) the quantity of gas puffed in the torus should not give rise to a pressure higher than 10^{-3} mbarl, to avoid activating security measures, foreseen in case of a leak.

Injecting 120 mbarl of gas we could observe that: 1) the rate of current quench is about 20

MA/s in the case of He puff and increases to 60 and 78 MA/s in the case of Ar and Ne puff; 2) the time of flight of the gas, from injector to plasma edge, is proportional to the square root of the atomic mass (as expected); 3) the increase of the line integrated density before disruption depends strongly on the sort of gas: the He, Ne and Ar puffs increase the line average density of a factor of 3, 2 and less than 0.5 respectively. This is probably a consequence of the different penetration length of Ar, Ne and He. The retention of Ar in the machine after impurity puff was higher than for Ne and He. Traces of Ne could barely be observed in discharges following strong gas puff; however in shots following Ar puff the fraction of the input power radiated was observed to be significantly higher than in the previous shot because of impurity contamination.

Due to 1) the smaller effect of He in accelerating the current quench, 2) the smaller sound velocity of Ar, 3) the higher Ar contamination of the next discharge with respect to Ne and He, it was decided to concentrate further the experiments with elongated plasmas on Ne. In a series of disruptions caused by density limit (800 kA, 1.5 and 2 Tesla,), the locked mode signal was used to trigger the fast valve and inject 30, 60 and 120 mbarl of Ne. The maximal force on the vessel, measured at 8 suspension rods decreased with the increase of the gas quantity from 190 kN down to 65 kN (see Fig. 5). The halo currents decreased in a similar way from 300 kA down to 120 kA. Their degree of asymmetry on a small scale did not change significantly with the injection of gas. We conclude that the injection of 120 mbarl of Ne and the reduction of 34 % of the forces on the vessel is a suitable mitigation scenario for ASDEX Upgrade.

The generation of runaway electrons (RE) have been observed in a few discharges with densities lower than $4 \ 10^{19} \ m^{-3}$ and magnetic field larger than 2 Tesla before and after thermal quench with the injection of Ar and Ne. Bursts in the SXR spatially and temporally localized are seen before and after thermal quench in plasmas with a higher density and without the generation of HXR emission,

5. Conclusions.

A clear m=1 n=1 perturbation of the halo current is seen in many ASDEX Upgrade disruptions; it is clearly correlated with q_{cyl} dropping below 2 and with a MHD event. The local degree of asymmetry of the halo current can be relatively large (tpf $\simeq$ 3.5).

Slow VDEs at large plasma current (1, 1.2 MA) cause vertical forces on the vessel comparable to the force associated with the statical weight of the vessel. The toroidal asymmetry of these measurements is around 10 %. The strain and displacement gauges have provided a database of measurements of good quality in the period 1-8.2002. The radial displacements of the vessel are significantly smaller (0.2 mm) than those observed in JET (7mm). The correlation between the relatively large (but localized) asymmetry of the halo currents and the absence of larger asymmetries in the vessel displacement still have to be carefully investigated.

The injection of 120 mbarl of Ne is a suitable scenario for the significant mitigation of forces in ASDEX Upgrade.

REFERENCES.

[1] G. Pautasso et al., Nuclear Fusion **42** (2002)

[2] Y. Nakamura et al., paper EX/P4-13 at this Conference

[3] G. Pautasso et al, Proc. 28th Eur. Conf. Madeira (2001)

[4] V. Riccardo et al., Plasma Phys. Control. Fusion **42** (2000) 29.

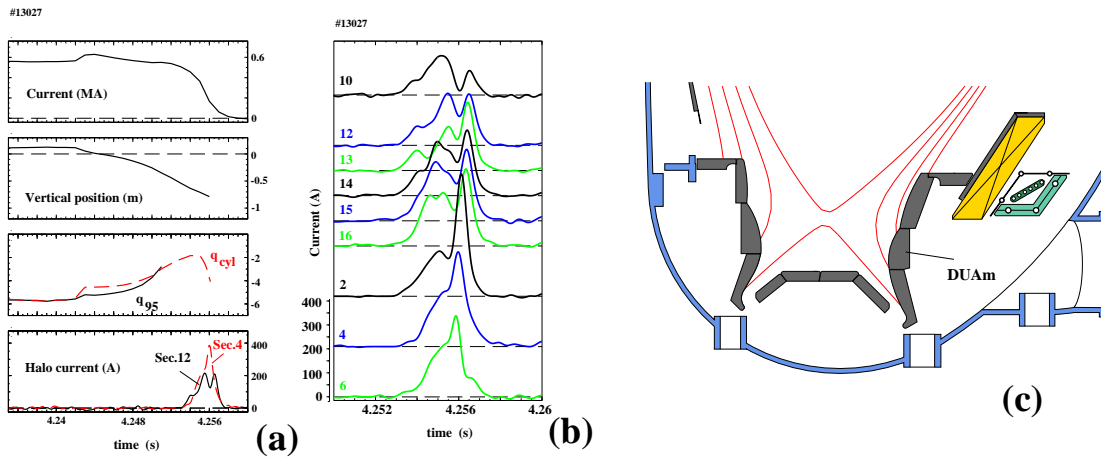[5] A. Savtchkov et al., Proc. 29th Eur. Conf. Montreux (2002)

Figure 1. (a) Time traces of several plasma parameters and of the halo current measurements at the DUAm tiles positioned 180 degree apart. (b) Time traces of the halo current measured at the 8 tiles of the DUAm (c) toroidal array in sector 10, 12, etc.
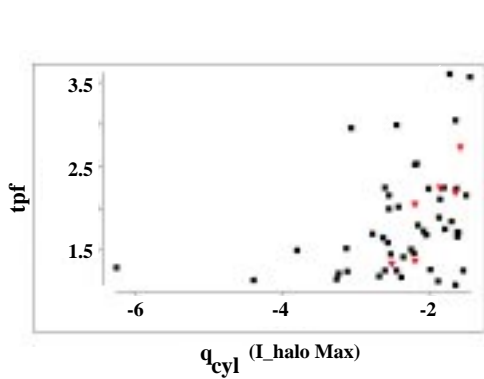

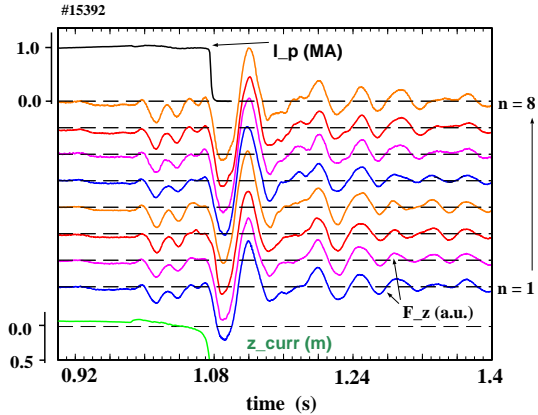Figure 2. Local toroidal peaking factor (tpf) versus q_cyl at maximum halo current.

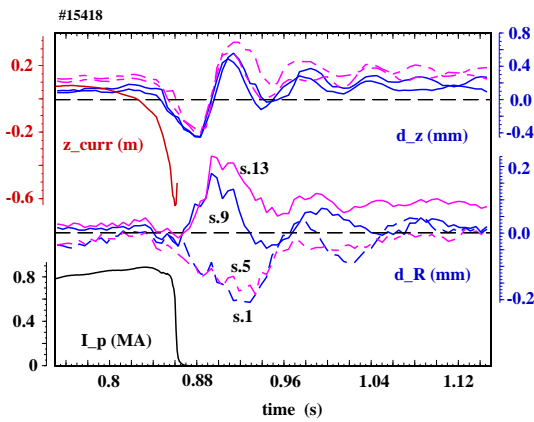Figure 3. Vessel displacement at the 8 suspension rods after VDE.

Figure 4.. Vertical (d_z) and radial (d_R) vessel displacement at the middplane after VDE.
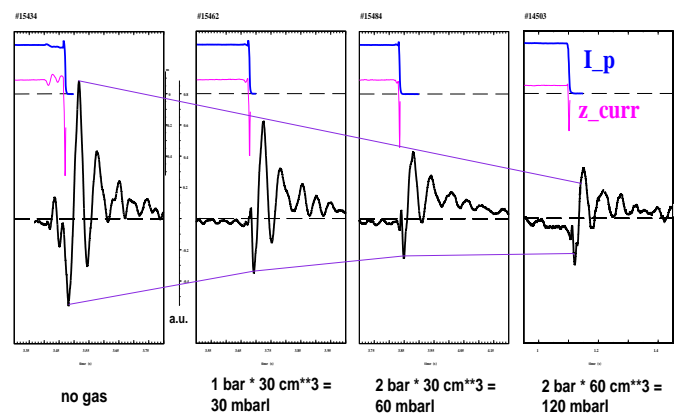

Figure 5. Reducton of the vertical forces on the vessel with puff of different amounts of Ne.